



ELSEVIER

Contents lists available at ScienceDirect

## Comptes Rendus Physique

www.sciencedirect.com



Cosmic inflation / Inflation cosmique

## Escher in the Sky

*Escher dans le ciel*

Renata Kallosh\*, Andrei Linde

Department of Physics and SITP, Stanford University, Stanford, CA 94305, USA

## ARTICLE INFO

## Article history:

Available online 25 August 2015

## Keywords:

Inflation  
Supergravity  
Geometry

## Mots-clés :

Inflation  
Supergravité  
Géométrie

## ABSTRACT

We give a brief review of the history of inflationary theory and then concentrate on the recently discovered set of inflationary models called cosmological  $\alpha$ -attractors. These models provide an excellent fit to the latest observational data. Their predictions  $n_s \approx 1 - 2/N$  and  $r \approx 12\alpha/N^2$  are very robust with respect to the modifications of the inflaton potential. An intriguing interpretation of  $\alpha$ -attractors is based on a geometric moduli space with a boundary: a Poincaré disk model of a hyperbolic geometry with the radius  $\sqrt{3\alpha}$ , beautifully represented by the Escher's picture Circle Limit IV. In such models, the amplitude of the gravitational waves is proportional to the square of the radius of the Poincaré disk.

© 2015 Académie des sciences. Published by Elsevier Masson SAS. All rights reserved.

## R É S U M É

Après une brève revue de l'histoire de la théorie de l'inflation, cet article introduit une classe de modèles inflationnaires récemment découverte : les « attracteurs de type  $\alpha$  ». Ces modèles offrent un très bon accord avec les données observationnelles. Leur prédiction sur l'indice spectral et le rapport tenseur-scalaire,  $n_s \approx 1 - 2/N$  et  $r \approx 12\alpha/N^2$ , est très robuste vis-à-vis d'une modification du potentiel de l'inflaton. Une interprétation surprenante de ces attracteurs  $\alpha$  repose sur la géométrie des espaces de modules avec bord : celle d'un disque hyperbolique de Poincaré de rayon  $\sqrt{3\alpha}$ , merveilleusement représenté par le dessin *Circle Limit IV* d'Escher. Dans ces modèles, l'amplitude des ondes gravitationnelles est proportionnelle au carré du rayon du disque de Poincaré.

© 2015 Académie des sciences. Published by Elsevier Masson SAS. All rights reserved.

## 1. Introduction

During the last 35 years, inflationary theory evolved from something that could look like a beautiful science fiction story to the well established scientific paradigm describing the origin of the universe and its large scale structure. Many of its predictions have been already confirmed by observational data, see e.g. [1,2]. And yet the development of this branch of science is not over. In this paper we will briefly remember the first steps of its development, and then relate them to a

\* Corresponding author.

E-mail addresses: [kallosh@stanford.edu](mailto:kallosh@stanford.edu) (R. Kallosh), [alinde@stanford.edu](mailto:alinde@stanford.edu) (A. Linde).

broad set of inflationary models which seem to fit observational data particularly well, and which make predictions nearly independent on the shape of their inflationary potentials. We called these theories “cosmological attractors.” As we will show, this class of models is closely related to some of the pioneering inflationary models such as the simplest versions of the chaotic inflation scenario [3,4] and the Starobinsky model [5]. But what makes these theories especially interesting is their geometric nature and supergravity realization, bringing us back to the discussion of the Poincaré disk and Escher’s paintings. To put these theories into proper context, we will remind here some basic facts from the history of development of inflationary models.

## 2. A brief history of inflationary ideas

The development of inflationary cosmology had more than a fair share of twists and turns, and it is very different from its first implementations. It took several years until the contours of this theory became sufficiently well established.

The first model of inflationary type was proposed by Starobinsky [5]. In its original form, it was based on adding the contribution of conformal anomaly to the Einstein theory, which required existence of enormous number of different types of elementary particles contributing to the anomaly. Instead of attempting to solve the homogeneity and isotropy problems, which is the defining feature of all inflationary models, Starobinsky assumed that the universe was homogeneous and isotropic from the very beginning, and emphasized that his scenario was “the extreme opposite of Misner’s initial chaos” [5]. The goal of the model was to solve the singularity problem by starting the evolution in a non-singular de Sitter state. However, dS state in his scenario was unstable, with a finite decay time [6], and therefore it could not exist at  $t \rightarrow -\infty$ .

The main goals of inflationary theory were formulated for the first time in the context of old and new inflation [7–9]. These models were based on an assumption that the universe initially was in a state of thermal equilibrium at an extremely high temperature, and then it supercooled and inflated in a state close to the top of the potential  $V(\phi)$ . At that time, this assumption seemed established beyond any reasonable doubt. However, old inflation did not quite work, as pointed out by its author [7], and it did not lead to perturbations of the cosmic microwave background radiation, which were predicted in [6,10] and discovered by COBE, WMAP and Planck. New inflation resolved most of the problems of old inflation, but it was also ruled out a year later, for many reasons discussed in [4]. After the first successes of inflationary theory, its future could appear quite bleak. As Hawking said in his book back in 1988, “the new inflationary model is now dead as a scientific theory, although a lot of people do not seem to have heard about its demise and write papers as if it were viable” [11].

The situation changed with the invention of the chaotic inflation scenario [3]. It was proposed as an alternative to new inflation, after it was realized that the assumption of the hot Big Bang, high temperature phase transitions and supercooling did not help to formulate a successful inflationary theory. In fact, these basic assumptions, the standard trademarks of old and new inflation, made inflation much more difficult to implement. If, instead, one simply considers the universe with different initial conditions in its different parts (or different universes with different values of fields in each of them), one finds that in many of them inflation may occur. It makes these parts exponentially large, thus producing exponentially large islands of order from the primordial chaos. Hence the name: chaotic inflation.

An important feature of this scenario is its versatility and the broad variety of models where it can be implemented. Examples of chaotic inflation models proposed in 1983–1985 included models with monomial and polynomial potentials, and any other models where the slow roll regime was possible. This regime is possible in small field models, with the potentials of the new inflation type, or with models with the Higgs-like potential  $\sim \lambda(\phi^2 - v^2)^2$  with  $v \gg 1$  [12]. Models of that type later have been called “hilltop inflation” [13]. Another example was the supergravity-based version of chaotic inflation with the potential  $V \sim a(1 - e^{-b\phi})$  [14], which originally appeared in the first realization of chaotic inflation in supergravity. In what follows we will call it the GL model. In 1983–1985, the Starobinsky model [5] experienced significant modifications. It was reformulated as a theory  $R + aR^2$ , and initial conditions for inflation in this theory were formulated along the lines of the chaotic inflation scenario [15–17]. This resolved the problem with initial conditions of the original version of this model. In the natural inflation scenario, the authors said that “our model is closest in spirit to chaotic inflation” [18]. The hybrid inflation scenario [19] was introduced as a specific version of the chaotic inflation scenario. Step by step, chaotic inflation replaced new inflation in its role of the main inflationary paradigm. Rather than describing some particular subset of inflationary models, it describes the most general approach to inflationary cosmology, which can easily incorporate ideas of quantum cosmology, eternal inflation, inflationary multiverse, and string theory landscape [20–33].

But this did not happen overnight. Chaotic inflation was so much different from old and new inflation that for a while it was psychologically difficult to accept. Even now, 30 years since the demise of old and new inflation, most of the college books on physics and astrophysics still describe inflation as exponential expansion in the false vacuum state during cosmological phase transitions with supercooling in Grand Unified Theories. That is why a significant part of the first book on inflation [4] was devoted to the discussion of new inflation versus chaotic inflation.

By now, this discussion is over, most of the existing models of inflation are based on the main principles of chaotic inflation. However this introduced a purely terminological issue: every new inflationary model belonging to the general class of chaotic inflation is introduced with its own name. That is why some authors invented a different classification of models and say, incorrectly, that chaotic inflation describes only models with monomial potentials, or only large field models, as opposite, e.g., to the hilltop inflation, natural inflation and hybrid inflation. In this paper we use the original definition of chaotic inflation following [3,4].

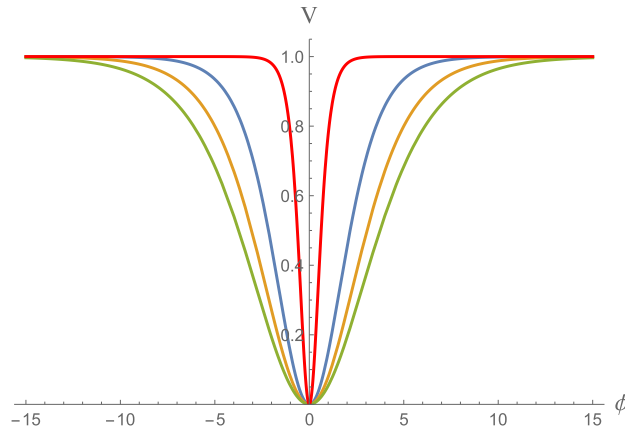


**Fig. 1.** (Color online.) Blue, brown and green lines show the potentials of the T-models with  $V \sim \tanh^2 \frac{\varphi}{\sqrt{6\alpha}}$  for  $\alpha = 1, 2, 3$  correspondingly. The red line in the center shows the potential of the GL model [14].

### 3. $\alpha$ attractors: T-models and E-models

Despite the generality of the chaotic inflation scenario described in the previous section, there is a good reason why in minds of many cosmologists chaotic inflation is often associated with the simplest model with a quadratic potential, with the Lagrangian [3,4],

$$\frac{1}{\sqrt{-g}}\mathcal{L} = \frac{1}{2}R - \frac{1}{2}\partial\phi^2 - \frac{1}{2}m^2\phi^2 \tag{1}$$

Nothing can be simpler than that, and yet it leads to inflation. This simplicity served as one of the main arguments in favor of naturalness of inflationary theory: No need for false vacuum states, complicated potentials and cosmological phase transitions with supercooling, just take a theory with a simple harmonic oscillator potential, put it into a cosmological background, and we are done.

However, the new observational data strongly suggest that this model predicts too large amplitude of gravitational waves, and therefore it requires modifications [1,2]. The simplest modification, which we are going to discuss in this paper, is provided by the models of cosmological  $\alpha$  attractors [34–40]. For example, one may consider a theory with the Lagrangian

$$\frac{1}{\sqrt{-g}}\mathcal{L}_T = \frac{1}{2}R - \frac{1}{2}\frac{\partial\phi^2}{(1 - \frac{\phi^2}{6\alpha})^2} - \frac{1}{2}m^2\phi^2 \tag{2}$$

The only thing that changed here as compared to (1) is the non-minimal kinetic term containing a parameter  $\alpha$  which can take any positive value. At  $\alpha \rightarrow \infty$  this model coincides with the simplest chaotic inflation model (1).

The field  $\phi$  is not canonically normalized. It must satisfy the condition  $\phi^2 < 6\alpha$ , so that the sign of the inflaton kinetic term is non-singular. But one can easily go to canonically normalized variables  $\varphi$ . For any finite  $\alpha$  one can solve equation  $\frac{\partial\phi}{1 - \frac{\phi^2}{6\alpha}} = \partial\varphi$ , which yields

$$\phi = \sqrt{6\alpha} \tanh \frac{\varphi}{\sqrt{6\alpha}} \tag{3}$$

The boundary of the moduli space  $\phi = \pm\sqrt{6\alpha}$  becomes  $\pm\infty$  in terms of the canonically normalized inflaton field  $\varphi$ , and the quadratic potential becomes  $V = 3\alpha m^2 \tanh^2 \frac{\varphi}{\sqrt{6\alpha}}$ . We called such  $\alpha$ -attractors ‘T-models’: their potentials depend on  $\tanh^2 \frac{\varphi}{\sqrt{6\alpha}}$ , they are symmetric with respect to the change  $\varphi \rightarrow -\varphi$  and look like letter T [34]. All potentials  $V(\phi^2)$  belong to the general class of T-models, which includes the GL model [14], which was the first successful implementation of chaotic inflation in supergravity. In modern language, GL model described  $\alpha$  attractor with  $\alpha = 1/9$  and the potential  $V(\phi) \sim \phi^2(1 - \frac{3}{8}\phi^2)$  [39,40] (Fig. 1).

In the leading order in the inverse number of e-foldings  $N$ , for  $\alpha \ll N$ , the slow roll parameters  $n_s$  and  $r$  for T-models are

$$1 - n_s = \frac{2}{N}, \quad r = \frac{12\alpha}{N^2} \tag{4}$$

For large  $\alpha$ , the prediction for  $n_s$  practically does not change, but the growth of  $r$  slows down:  $r \approx \frac{12\alpha}{N(N+3\alpha/2)}$  [36]. The exact interpolating values of  $n_s$  and  $r$  for the theory  $V = \tanh^2 \frac{\varphi}{\sqrt{6\alpha}}$  are plotted in Fig. 2 by a thick purple vertical line

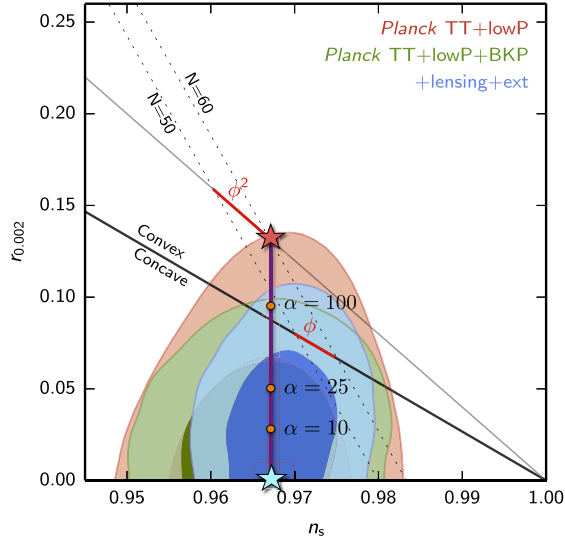


**Fig. 2.** (Color online.) Predictions of the simplest  $\alpha$ -attractor T-model with the potential  $V \sim \tanh^2 \frac{\phi}{\sqrt{6\alpha}}$  for  $N = 60$  cut through the most interesting part of the Planck 2015 plot for  $n_s$  and  $r$  [2].

superimposed with the results for  $n_s$  and  $r$  from the Planck 2015 data release [2]. This line begins at the point corresponding to the predictions of the simplest quadratic model  $\frac{m^2}{2}\phi^2$  for  $\alpha > 10^3$  (red star), and then, for  $\alpha \lesssim 40$ , it enters the region most favored by the Planck data. For  $\alpha = 1$ , these models give the same prediction  $r \sim 12/N^2$  as the Starobinsky model, the Higgs inflation model [41], and the broad class of superconformal attractors [34]. Then the same vertical line continues further down towards the prediction  $r \sim 4/3N^2$  of the GL model [14,39] corresponding to  $\alpha = 1/9$ . Then it goes even further, all the way down to  $r \rightarrow 0$  in the limit  $\alpha \rightarrow 0$ . Predictions of all models with  $\alpha \lesssim O(1)$  are so close to each other, that they are covered by the same blue star in Fig. 2.

One can show that in the large  $N$  limit not only  $n_s$ , but also the amplitude of scalar perturbations in this class of models does not depend on  $\alpha$ ; it depends only on  $N$  and  $\mu$ . For  $N = 60$ , this amplitude matches the Planck 2015 normalization if  $\mu \approx 10^{-5}$ .

Moreover, for sufficiently small  $\alpha \lesssim O(1)$ , the predictions of  $\alpha$ -attractors in the large  $N$  limit almost do not depend on whether we take the potential  $\tanh^2 \frac{\phi}{\sqrt{6\alpha}}$ , or use a general class of potentials  $V(\phi) = f^2(\phi) = f^2(\tanh \frac{\phi}{\sqrt{6\alpha}})$  for a rather broad set of choices of the functions  $f(\phi)$ . This stability of predictions, as well as their convergence to one of the two attractor points shown in Fig. 2 by the red and blue stars, is the reason why we called these theories the cosmological attractors. The latest Planck 2015 result  $n_s = 0.968 \pm 0.006$  [2] almost exactly coincides with the prediction of the simplest T-models for  $N = 60$ . These properties of T-models are quite striking. Since their predictions can match any value of  $r$  from 0.14 to 0, see Fig. 2, these models may have lots of staying power.

As an example of a set of  $\alpha$  attractors corresponding to a slightly more complicated choice of the function  $f(\phi)$ , we will describe now a set of models with  $V(\phi) = f^2(\phi) = \left(\frac{\phi}{1+\phi/\sqrt{6\alpha}}\right)^2$ :

$$\frac{1}{\sqrt{-g}}\mathcal{L}_E = \frac{1}{2}R - \frac{1}{2}\frac{\partial\phi^2}{(1-\frac{\phi^2}{6\alpha})^2} - \frac{1}{2}m^2\frac{\phi^2}{(1+\frac{\phi}{\sqrt{6\alpha}})^2} \tag{5}$$

We called this set of  $\alpha$  attractors ‘E-models’ because the potential of these models has an explicit exponential dependence on the canonically normalized field  $\varphi$ , asymmetric with respect to the change  $\varphi \rightarrow -\varphi$ :  $V \sim (1 - e^{-\sqrt{\frac{2}{3\alpha}}\varphi})^2$ . In the special case  $\alpha = 1$  this potential coincides with the potential of the Starobinsky–Whitt model [15–17], which represents this model as a member of the general class of  $\alpha$ -attractors, see Fig. 3. The predictions of these models are shown in Fig. 4.

All of these models have the same kinetic term but different potentials. They have two common features. Generically, they have two attractor points, shown by the red and blue stars in Figs. 2 and 4, describing the limiting behavior for  $\alpha \rightarrow \infty$  and  $\alpha \rightarrow 0$ . More importantly, for sufficiently small  $\alpha$  (i.e. in the limit when the size of the moduli space becomes small) their cosmological predictions are very stable with respect to even very significant modifications of the potentials.

This property was explained in [34–36], and it was formulated in a particularly general way in [38]: The kinetic term in this class of models, as well as in many other models of cosmological attractors, has a pole near the boundary of the moduli space. If inflation occurs in a vicinity of such a pole (which happens for sufficiently small  $\alpha$ ), and the potential near the pole can be well represented by its value and its first derivative near the pole, all other details of the potential far away from the pole (from the boundary of the moduli space) become unimportant for making cosmological predictions. In particular, the spectral index depends solely on the order of the pole, while the tensor-to-scalar ratio also involves the residue [38]. All

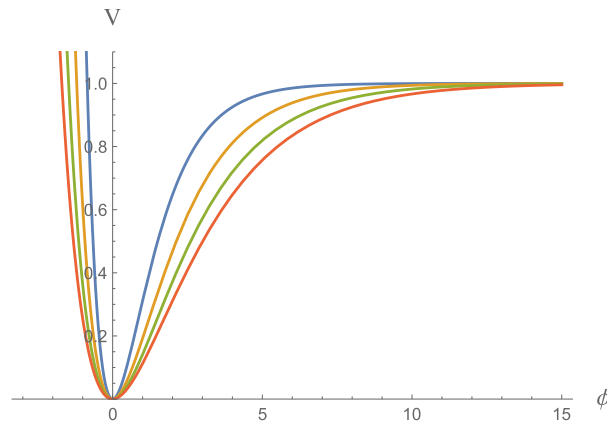


**Fig. 3.** (Color online.) E-model potential  $\alpha\mu^2(1 - e^{-\sqrt{\frac{2}{3\alpha}}\phi})^2$  in units of  $\alpha\mu^2 = 1$  for  $\alpha = 1, 2, 3, 4$ . Smaller  $\alpha$  correspond to more narrow minima of the potentials. The blue line shows the potential of the Starobinsky model, which belongs to the class of E-models with  $\alpha = 1$ .

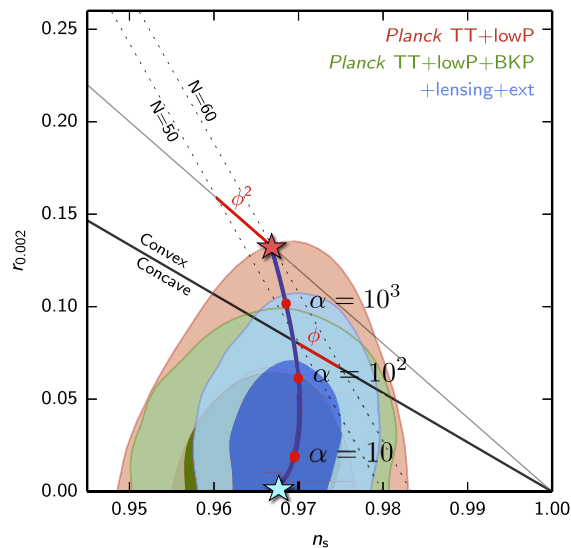


**Fig. 4.** (Color online.) Predictions of E-models with  $V \sim (1 - e^{-\sqrt{\frac{2}{3\alpha}}\phi})^2$ .

the rest is practically irrelevant, as long as the field after inflation falls into a stable minimum of the potential with a tiny value of the vacuum energy and stays there.

From the point of view of constructing single field inflationary models, everything becomes nearly trivial: Take any model with a pole in the kinetic term and a potential which has a minimum, and we are done, independently of many other details of the theory, in perfect agreement with observations. In this sense, everything becomes as transparent as in the simplest chaotic inflation model (1), but more general and stable with respect to the choice of the inflationary potential. One may argue that what this new class of models does for inflation is somewhat similar to what inflation did for cosmology. Inflation makes the structure of the observable part of the universe very stable with respect to the choice of initial conditions in the early universe. Meanwhile the cosmological attractors make inflationary predictions which are very stable with respect to the choice of the inflaton potential.

But can we implement this scenario in models related to advanced theories of fundamental interactions? And if the properties of the kinetic term are so important, is it possible that this class of models may have some interesting interpretation in terms of geometry of the moduli space? The rest of the paper will be dedicated to the discussion of these issues, under the guidance of Poincaré and Escher, as well as of many of our friends in the supergravity/string theory community.

#### 4. The hyperbolic plane $\mathbb{H}^2$

In the previous sections we briefly described an interpretation of  $\alpha$ -attractors in simple phenomenological models of a single scalar field. However, the main goal of this paper is to show that the parameter  $\alpha$  in advanced cosmological attractor models based on supergravity is best described by a size of the Poincaré disk famously represented by the Escher's Circle

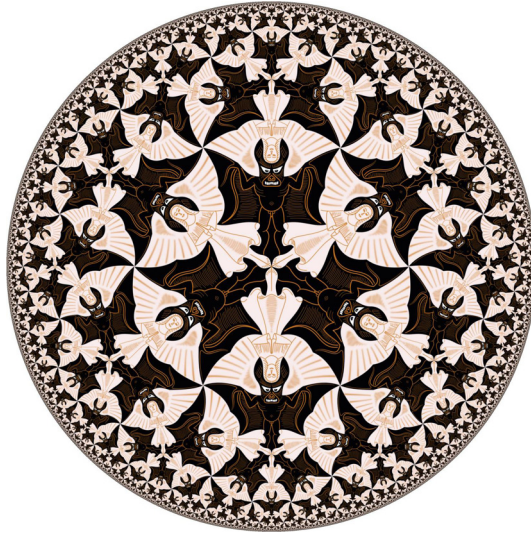


**Fig. 5.** (Color online.) A computer generated version of Escher’s picture Circle Limit IV (Heaven and Hell) by V. Bulatov, <http://bulatov.org/math/1201/>. It presents a Poincaré disk model of a hyperbolic geometry. The radius square of the disk in the context of our cosmological models is  $R^2 = 3\alpha$ . The curvature of this manifold  $\mathcal{R}_{\mathbb{H}^2} = -\frac{2}{3\alpha}$ . To see angels and devils moving in the Poincaré disk click here: <http://youtu.be/milmZUVSjro>.

Limit IV, see Fig. 5. Namely, the radius square of the boundary of this circle  $R^2$ , in the context of our cosmological models, is given by  $3\alpha$ . The smaller the level of primordial gravity waves, the smaller the circle! Current data implies that  $R^2 \lesssim 75$  for the simplest T-model and  $R^2 \lesssim 300$  for the simplest E-model.

The hyperbolic plane  $\mathbb{H}^2$  has a long history in mathematics and physics, see for example [42]. The Poincaré disk model of a hyperbolic geometry is presented by the Escher’s picture Circle Limit IV, see Fig. 5. The boundary circle (which is not part of the hyperbolic plane) is called the *absolute*. One can place an infinite amount of angels and devils, of the size which looks decreasing, towards the boundary in this circle, as Escher did. However, in fact, the correct understanding of hyperbolic geometry means that the angels and devils close to the boundary are of the same ‘physical’ size as the ones near the center of the circle. How do we explain this? As always in a curved space the concept of a distance (or size) depends on the geometry and there is a difference between the coordinate distance and physical distance.

The moduli space metric of these models, associated with the kinetic term of the scalars field is

$$d^2s = \frac{1}{2} \frac{\partial^2 \phi}{(1 - \frac{\phi^2}{6\alpha})^2} = \frac{d^2r}{(1 - \frac{r^2}{3\alpha})^2} \tag{6}$$

Here  $r = \phi/\sqrt{2}$ . It may be viewed as a slice at a fixed angular direction of the 2d metric of the Poincaré disk:

$$d^2s = \frac{d^2r + r^2 d^2\theta}{(1 - \frac{r^2}{3\alpha})^2}, \quad r^2 < 3\alpha \tag{7}$$

A Poincaré disk is a space with a constant negative curvature  $\mathcal{R}_{\mathbb{H}^2} = -\frac{2}{3\alpha}$ . At  $\theta = \text{const}$ , this is a slice of the Escher’s picture, at fixed angular direction. Note that the physical distance on the hyperbolic disk is

$$d\rho = \frac{dr}{1 - \frac{r^2}{3\alpha}} \tag{8}$$

When  $\rho \rightarrow \infty$ ,  $r \rightarrow 3\alpha$ , towards the absolute, towards the boundary. When  $\theta$  is not fixed (not stabilized by a dynamical mechanism during the cosmological evolution) the supergravity  $\alpha$ -attractor models actually have a kinetic term for scalars presenting a Poincaré disk model of a hyperbolic geometry in Eq. (7), as we will show in a more technical Section 5.

At this point a cosmologist might ask a question: why do we have to start with the complicated inflaton kinetic term shown in (2), (5) which we call here a moduli space? A simple answer to this question is: we have assumed that our  $\alpha$ -models have a certain symmetry, called Möbius symmetry. It is a generic symmetry of superconformal theories. We show the picture associated with this symmetry, in Fig. 6, Escher’s type picture of Circle Limit III.

### 5. Relation to negatively curved 3-geometries in FRW metric

It is important to stress here that the metric of the moduli space in (2), where the scalar fields are coordinates of the manifold, is not a metric of the space-time. In (6) we name the coordinate  $r$  instead of  $\phi/\sqrt{2}$  only for the purpose of

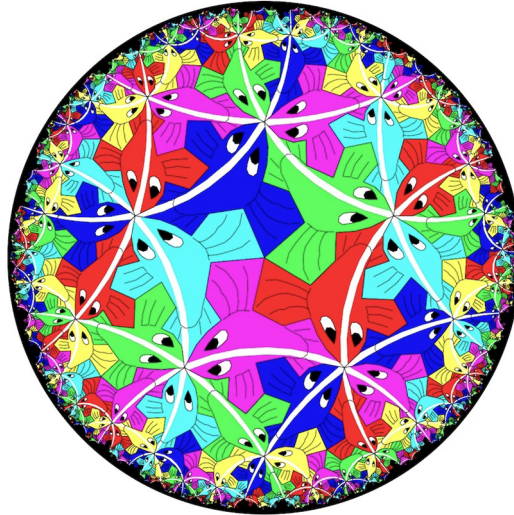


**Fig. 6.** (Color online.) A computer-generated picture by D. Dunham inspired by Escher's picture Circle Limit III, <http://www.math-art.eu/Documents/pdfs/Dunham.pdf>. It presents a Poincaré disk model of a hyperbolic geometry. The symmetries of the geometry are shown here via configuration of fishes and how these configurations are mapped into other parts of a space. Mathematically, we will explain the symmetry in Section 7.

inviting an intuition gained in general relativity with regard to space-time geometry, to be used for the geometry of the moduli space, where coordinates are scalar fields.<sup>1</sup>

In fact, the space of a constant negative curvature, which is a Poincaré disk model of a hyperbolic geometry, reminds the 3d slice at constant time of the familiar FRW geometry in case of the open universe with  $k = -1$ . It is known that the 2d slice of the open FRW universe is related to Escher's picture Circle Limit IV, see e.g. [44]. Observationally at present our 3d geometry is very close to flat with  $k = 0$ . The corresponding parameter  $\Omega_K$  is given by [2],

$$\Omega_K = 0.000 \pm 0.005 \tag{9}$$

It appears that at present there is no indication that in our universe with the FRW model there is a negatively curved 3-geometry. However, more precise observations will take place in the future.

Meanwhile, the  $\alpha$ -models suggest a possibility of measuring the value of the curvature of a negatively curved 2-geometry not of a FRW model of a space and time but of the moduli space of scalars, which form a non-trivial geometry.

### 6. Supergravity $\alpha$ -attractor models with disk geometry

Generic supergravity models are described by superfields and Kähler geometry. It means that the complex scalars are coordinates of the Kähler manifold. In the simplest case of the  $\alpha$ -attractor models we will focus only on the inflaton superfield  $Z = z(x) + ia(x)$ . The corresponding Kähler geometry can be described as a disk geometry defined by a Kähler potential of the form  $K = -3\alpha \log(1 - Z\bar{Z})$  where  $Z\bar{Z} < 1$ . The moduli space metric is defined as

$$d^2s = g_{Z\bar{Z}} dZ d\bar{Z}, \quad g_{Z\bar{Z}} = K_{Z\bar{Z}} = \frac{3\alpha}{(1 - Z\bar{Z})^2} \tag{10}$$

Formally, we may proceed by a computation of the Kähler manifold curvature using the definition of it via the metric:

$$\mathcal{R}_{\text{Kähler}} = -g_{Z\bar{Z}}^{-1} \partial_Z \partial_{\bar{Z}} \log g_{Z\bar{Z}} = -\frac{2}{3\alpha} \tag{11}$$

This is not quite illuminating, so we may try to do better using the Escher's Circle Limit picture. A very nice interpretation of  $\alpha$  in (10) and in (11) comes from the concept of the Poincaré disk model of a hyperbolic geometry, as we pointed out around Eq. (6). First we establish that our disk Kähler geometry is actually a Poincaré disk model of a hyperbolic geometry

$$d^2s = \frac{3\alpha}{(1 - Z\bar{Z})^2} dZ d\bar{Z} = \frac{d^2x + d^2y}{\left(1 - \frac{x^2 + y^2}{3\alpha}\right)^2} \tag{12}$$

<sup>1</sup> The importance of moduli spaces of a constant negative curvature in type IIA compactification of string theory for constructions of de Sitter vacua and cosmological inflationary models was stressed in [43].

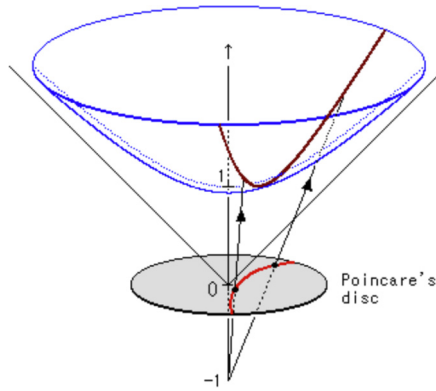


**Fig. 7.** (Color online.) A unit size hyperboloid given in Eq. (19), see Wikipedia for Poincaré disk model. In this picture the Poincaré disk model is a perspective projection viewed from the point  $w = -1, u = v = 0$  projecting the upper half hyperboloid onto a  $u, v$  disk of at  $w = 0$ . The red circular arc is geodesic in Poincaré disk model; it projects to the brown geodesic on the blue hyperboloid. The figure shows the Poincaré disk of a radius  $R = \sqrt{3\alpha} = 1$ .

where  $Z = (x + iy)/\sqrt{3\alpha}$ . We have shown this geometry in polar coordinates in Eq. (7). The physical distance in this geometry is defined by  $d\rho = \frac{dr}{1-\frac{r^2}{3\alpha}}$ , and we find that

$$r = \sqrt{3\alpha} \tanh \frac{\rho}{\sqrt{3\alpha}} \tag{13}$$

When  $\rho \rightarrow \infty$ ,  $r$  never reaches  $3\alpha$  since  $\tanh < 1$ . The curvature of the Poincaré disk of a radius  $R = \sqrt{3\alpha}$  is equal to  $-2/R^2$

$$\mathcal{R}_{\text{Poincaré}} = -\frac{2}{3\alpha} \tag{14}$$

Finally, we can convert our geometry into a well known metric of an open 2d universe with a negative curvature  $R_{\text{open}} = -\frac{2}{3\alpha}$

$$d^2s = \frac{3\alpha}{(1 - Z\bar{Z})^2} dZ d\bar{Z} = \frac{3\alpha}{4} (d^2\chi + \sin^2 \chi d^2\theta) \tag{15}$$

where the following change of variables was performed

$$Z = e^{i\theta} \tanh \frac{\chi}{2} \tag{16}$$

Note that the relation between  $\chi$  and a canonical field  $\varphi$  is given by

$$\frac{\chi}{2} = \frac{\varphi}{\sqrt{6\alpha}} \tag{17}$$

A complementary point of view on this geometry is given by a Minkowski metric in the embedding 3d space

$$d^2s = \frac{1}{4} (d^2u + d^2v - d^2w) \tag{18}$$

where the coordinates are restricted to a hyperboloid. This hyperboloid is associated with the negative space curvature (and an open universe, when the geometry is a part of FRW metric).

$$-u^2 - v^2 + w^2 = 3\alpha \tag{19}$$

If we resolve this condition by taking

$$\begin{aligned} u &= \sqrt{3\alpha} \sinh \chi \cos \theta \\ v &= \sqrt{3\alpha} \sinh \chi \sin \theta \\ w &= \sqrt{3\alpha} \cosh \chi \end{aligned} \tag{20}$$

with  $0 \leq \chi < \infty$  and  $0 \leq \theta \leq 2\pi$  we recover the geometry in Eq. (15) and the upper part of the hyperboloid in Fig. 7. An artistic version of it is shown in Fig. 7. In our case we have a geometry based on one complex scalar, which plays a role of coordinates in the moduli space.



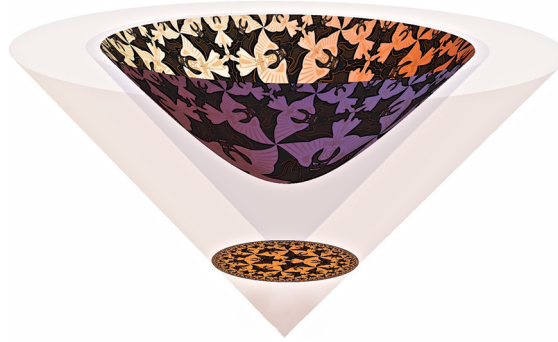


**Fig. 8.** (Color online.) An artistic version of Fig. 7, which shows that angels and devils crowded near the boundary of the Poincaré disk have an open space on the hyperboloid, when projected from the disk.



**Fig. 9.** (Color online.) Escher’s picture of a Heaven and Hell in half-plane variables, due to V. Bulatov. The boundary of the half-plane  $T + \bar{T} \rightarrow 0$  is the absolute which cannot be reached. The angels and devils look smaller and smaller near the boundary.

**7. Superconformal  $\alpha$ -attractor models: Escher’s Circle and Escher’s Half-Plane**

The disk geometry is described by a complex variable  $Z$  such that  $Z\bar{Z} < 1$ . A half-plane geometry in  $T$  variables with  $T + \bar{T} > 0$  is related to it by a change of variables [37]

$$Z = \frac{T - 1}{T + 1}, \quad T = \frac{1 + Z}{1 - Z} \tag{21}$$

The corresponding disk geometry is presented by Escher’s Circle Limit IV in Fig. 5, and a Half-Plane one by an Escher’s Half-Plane in Fig. 9. Same for Escher’s Circle Limit III in Figs. 7 and 8, and a Half-Plane one in Fig. 10.

The analysis of cosmological  $\alpha$ -models of inflation in disk and half-plane variables was performed in [36,37]. The generalized cosmological  $\alpha$  models of inflation and dark energy with susy breaking, in disk and half-plane variables, were introduced in [40]. A detailed analysis of stability of these models will be presented in [45].

The Kähler potential in half-plane coordinates is  $K = -3\alpha \log(T + \bar{T})$ . The curvature of the Kähler manifold is computed using the Kähler metric  $d^2s = g_{T\bar{T}} dT d\bar{T}$  with  $g_{T\bar{T}} = K_{T\bar{T}} = \frac{3\alpha}{(T + \bar{T})^2}$ :

$$\mathcal{R}_{\text{Kähler}} = -g_{T\bar{T}}^{-1} \partial_T \partial_{\bar{T}} \log g_{T\bar{T}} = -\frac{2}{3\alpha} \tag{22}$$

Since the relation between the disk and half-plane is due to a change of coordinates  $Z = \frac{T-1}{T+1}$ , it is not surprising that the curvature in the half-plane coordinates is the same as in the disk ones.

An alternative form of this negative constant curvature space associated with Figs. 9, 10 can be also given in terms of the constant scalar curvature metrics on toric manifolds [50]. The scalar curvature for the metrics on toric manifolds is

$$d^2s = \frac{3\alpha}{y^2} d^2y \Rightarrow \mathcal{R}_{\text{toric}} = -\left[\frac{1}{g(y)}\right]'' = -\frac{2}{3\alpha} \tag{23}$$

where  $u(y)$  is its symplectic potential and  $g = u''$ .

In all cases we find the same result for the curvature:  $\mathcal{R} = -\frac{2}{3\alpha}$ , but the Escher’s circle limit pictures in Fig. 5 and Fig. 7 help us to provide a simple interpretation of the parameter  $\alpha$ . It will eventually be measured (or bounded) in the context of the  $\alpha$ -attractor models, by looking at the primordial gravity waves from the sky (Fig. 2 and Fig. 4).

The origin of the Poincaré disk model and of a half-plane geometry in supergravity models of the  $\alpha$ -attractors can be traced back to studies of  $\mathcal{N} = 4$  supergravity in [46], where it was shown that the disk action for the moduli  $\frac{\partial Z \partial \bar{Z}}{(1 - Z\bar{Z})^2}$  has an  $SU(1, 1)$  symmetry. They have also explained that for  $\mathcal{N} = 1$  supergravity a more general class of models with  $3\alpha \frac{\partial Z \partial \bar{Z}}{(1 - Z\bar{Z})^2}$  still has an  $SU(1, 1)$  symmetry for an arbitrary  $\alpha$ . The same symmetry was also discovered in a maximal superconformal

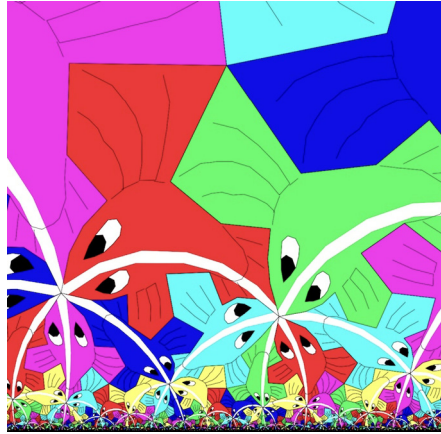


**Fig. 10.** (Color online.) A computer generated picture by D. Dunham, <http://www.math-art.eu/Documents/pdfs/Dunham.pdf>, representing a half-plane geometry version of Fig. 6.

model [47] which has a local  $SU(4) \times U(1)$  symmetry and a global  $SU(1, 1)$  symmetry. Upon gauge-fixing some of the superconformal symmetries it becomes an  $\mathcal{N} = 4$  supergravity with the remaining  $SU(1, 1)$  symmetry. With one choice of a gauge [47] one finds a disk geometry with  $Z$ -variables,  $Z\bar{Z} < 1$ , the absolute is given by equation  $Z\bar{Z} = 1$ . With the other choice one finds a geometry of the half-plane, with  $T$ -variables,  $T + \bar{T} > 0$ , the boundary is at  $T + \bar{T} = 0$ . See [48], Eqs. (35) and (39) there, explaining both choices. These two choices are shown limit circles in Figs. 5, 7 and in half-plane ones in Figs. 9, 10.

The relation between these two geometries corresponds to a different choice of a local  $U(1) \mathbb{R}$ -symmetry gauge in the superconformal theory, [48]. On the other hand, a simple change of variables preserving the geometry  $d^2s$  was explained for our attractor models in [37] via a Cayley transform (21).

An origin of *manifolds with boundaries* can be traced also to the coset space structure of extended supergravities. For example in maximal  $\mathcal{N} = 8$  supergravity, with scalars in the coset space  $\frac{E_{7,7}}{SU(8)}$ , the positivity of kinetic terms of these scalars requires a condition [49], which upon truncation to  $\mathcal{N} = 4$  supergravity becomes  $Z\bar{Z} < 1$  with  $3\alpha = 1$ .

We may start with maximal  $\mathcal{N} = 4$  superconformal model and gauge-fix some local symmetries, including the Weyl symmetry [47,48], or perform a supersymmetric truncation of the maximal  $\mathcal{N} = 8$  supergravity [49]. For pure  $\mathcal{N} = 4$  supergravity we recover in both cases the following bosonic action, see for example Eq. (A.1) in [49]:

$$\frac{1}{\sqrt{-g}} \mathcal{L}_{\mathcal{N}4} = \frac{1}{2} R - \frac{dZ d\bar{Z}}{(1 - Z\bar{Z})^2} + \frac{1}{4} F_{\mu\nu}^{ab} F^{\mu\nu cd} \mathcal{M}_{abcd}(Z, \bar{Z}) \tag{24}$$

There is no potential, the kinetic term of the scalar  $Z$  represents a unit radius Escher disk geometry, the scalars interact with vectors  $F_{\mu\nu}^{ab}$ . For inflationary period (but not for the reheating stage) we may ignore vectors. If we were to associate this bosonic model with  $\mathcal{N} = 1$  supergravity, we would qualify it as  $K = -3\alpha \ln(1 - Z\bar{Z})$  with  $\alpha = 1/3$  and  $W = 0$ .

### 8. Isometries of the half-plane and the disk geometries

Here we focus on symmetries of our geometries. It involves the  $GL(2, \mathbb{R})$  Möbius transform. A simple form of it is given in terms of  $\tau$  variables, familiar to a string theorist, where  $\tau = iT$ . Namely, our half-plane geometry is given by

$$d^2s = 3\alpha \frac{dT d\bar{T}}{(T + \bar{T})^2} = 3\alpha \frac{d\tau d\bar{\tau}}{(2 \operatorname{Im} \tau)^2} \tag{25}$$

It is invariant under the transformations  $\tau \rightarrow \tau'$ , where

$$\tau' = \frac{a\tau + b}{c\tau + d}, \quad ad - bc \neq 0 \tag{26}$$

where  $a, b, c, d$  are real numbers and

$$\frac{d\tau d\bar{\tau}}{(\tau - \bar{\tau})^2} = \frac{d\tau' d\bar{\tau}'}{(\tau' - \bar{\tau}')^2} \tag{27}$$

Note that the  $GL(2, \mathbb{R})$  isometry of the half-plane is valid for  $ad - bc \neq 0$  and does not require that  $ad - bc = 1$ , which corresponds to an  $SL(2, \mathbb{R})$  symmetry. Thus the isometry is a general linear group over  $\mathbb{R}$  and includes a special linear group over  $\mathbb{R}$ . The symmetry is valid for any  $\alpha$ ; it defines the geometry of the moduli space that we are employing.



**Fig. 11.** (Color online.) The simplest quadratic inflationary potential  $V(Z, \bar{Z}) = \mu^2 Z \bar{Z}$  in the theory (32). The picture reveals the fact that the potential depends on disk coordinates with  $Z\bar{Z} < 1$  and the angels and devils are crowded near the top of the potential close to the boundary at  $|Z| = 1$ .

An analogous symmetry acts on the disk geometry. This is a Möbius transform of a Poincaré disk:

$$Z' = \frac{\beta Z + \gamma}{\bar{\gamma} Z + \bar{\beta}}, \quad |\beta|^2 - |\gamma|^2 > 0 \tag{28}$$

Here  $\beta$  and  $\gamma$  are complex numbers. The symmetry is the same, the properties of the geometry are the same for all  $\alpha$ , however, the size of the Escher’s Limit Circle is different, its radius square is  $3\alpha$ . In the context of our  $\alpha$ -attractor models we will measure  $\alpha$  when the primordial gravity waves will be discovered.

Some special choices for  $\alpha$  are:  $\alpha = 1/3$  and a unit size Escher disk  $R = 1$  correspond to a maximal  $\mathcal{N} = 4$  superconformal model and pure  $\mathcal{N} = 4$  supergravity,  $r \sim 10^{-3}$ . The case  $\alpha = 1$  and an Escher disk  $R = 3$  support the geometry of the  $\mathcal{N} = 1$  superconformal model,  $r \sim 3 \cdot 10^{-3}$ . Finally,  $\mathcal{N} = 1$  supergravity geometry is consistent with an arbitrary positive  $\alpha$ .

### 9. From moduli space to cosmology

Until now, we focused on the geometry of the moduli space, described by the kinetic term in the Lagrangian. There was a good reason to do it: Once we decide on a potential, we can study the evolution of the observable universe, and compare it with the data in [1,2], and especially with the future data. There are many options with regard to the choice of a potential.

A generic class of inflationary models [40] compatible with the current data, as well as capable of describing dark energy and controllable susy breaking, involve an addition chiral superfield  $S$ , which can be arranged to vanish during and after inflation. The corresponding Kähler potential is now

$$K = -3\alpha \ln(1 - Z\bar{Z} - S\bar{S}) \tag{29}$$

and in the context of  $\mathcal{N} = 1$  supergravity we can make a choice of a holomorphic superpotential  $W = A(Z) + SB(Z)$ .

A very simple choice here comes from the  $\mathcal{N} = 4$  model (24), which suggests to use  $3\alpha = 1$ . We also take a very simple superpotential  $A(Z) = 0$  and  $B(Z) = \mu$ :

$$K = -\ln(1 - Z\bar{Z} - S\bar{S}), \quad W = \mu S \tag{30}$$

This leads to the theory with the bosonic action

$$\frac{1}{\sqrt{-g}} \mathcal{L}_{\mathcal{N}4 \rightarrow \mathcal{N}1} = \frac{1}{2} R - \frac{dZ d\bar{Z}}{(1 - Z\bar{Z})^2} - \mu^2 \tag{31}$$

This bosonic model has an embedding into  $\mathcal{N} = 1$  supergravity, according to (30). It also has an unbroken the Möbius symmetry (28). Its moduli space is the Poincaré disk with unit radius  $R = 1$ . And, from the point of view of cosmology, it describes de Sitter space with a positive vacuum energy  $V = \mu^2$  and spontaneously broken  $\mathcal{N} = 1$  supersymmetry. Thus we are coming very close to describing inflation. We have dS space, but now we must find a way to end the stage of the exponential expansion in dS vacuum.

As a next step, we consider the same model but with the superpotential  $W = \mu SZ$ . This brings the action to the form closely resembling the simplest toy model (2) we started with:

$$\frac{1}{\sqrt{-g}} \mathcal{L}_{\mathcal{N}4 \rightarrow \mathcal{N}1} = \frac{1}{2} R - \frac{dZ d\bar{Z}}{(1 - Z\bar{Z})^2} - \mu^2 Z\bar{Z} \tag{32}$$

This model has a simple quadratic potential with respect to the complex field  $Z$ . However, in the theory (31) the value of the potential was everywhere the same across the Poincaré disk, whereas in (32) it approaches its maximum value close to the boundary of the moduli space at  $|Z| = 1$ , as shown in Fig. 11. As one can easily see, most of the angels and devils live close to this boundary. It could seem that they do not have much space here, and they should quickly fall down instead of hanging up in the sky. But this is not the case.

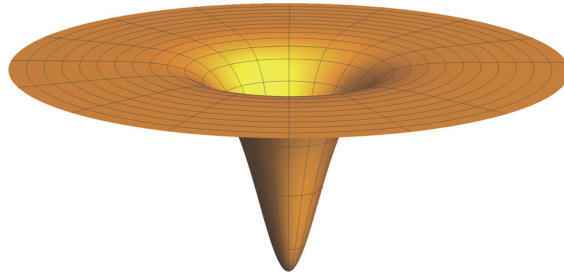


**Fig. 12.** (Color online.) Inflationary potential  $V$  in the theory (32), (33) with the radial direction represented by the canonical field  $\varphi$  with  $V \sim \tanh^2 \frac{\varphi}{\sqrt{2}}$ .

Indeed, if we represent the radial component in terms of the canonical field  $\varphi$ , as in Eq. (16),  $Z = e^{i\theta} \tanh \frac{\varphi}{\sqrt{2}}$ , our action (32) becomes

$$\frac{R}{2} - \frac{1}{2} \left( d^2\varphi + \frac{1}{2} \sinh^2(\sqrt{2}\varphi) d^2\theta \right) - \mu^2 \tanh^2 \frac{\varphi}{\sqrt{2}} \tag{33}$$

When  $|Z|$  approaches the boundary of the moduli space, the canonical field  $\varphi$  runs to infinity. This means, in effect, that the upper part of the paraboloid shown in Fig. 11 becomes infinitely stretched out, and this part of the potential becomes exponentially flat, as shown in Fig. 12, with the height of the plateau asymptotically approaching the vacuum energy  $\mu^2$  in dS space described by (31).

Fig. 12 does not give full justice to the volume of the moduli space at the plateau of the potential, because with the growth of the canonical field  $\varphi$ , shown by the circles, the distance in the angular direction grows exponentially fast, as  $\sinh(\sqrt{2}\varphi)$ , see (33). Therefore most of this volume is at indefinitely large values of the field  $\varphi$ . In other words, in accordance with this model, almost all angels and demons live at this high plateau.

This provides perfect initial conditions for inflation: Independently of the initial velocity of the scalar fields, their kinetic energy rapidly dissipates due to the cosmological evolution, the fields freeze at some point of the infinitely large plateau, until the exponentially slow descent in the radial direction towards the minimum of the potential shown in Fig. 12 begins. Unless one makes an unusual assumption that the decay rates of the radial and angular components of the field are dramatically different from each other, the perturbations of metric produced during inflation in this theory have the same properties as the perturbations in the simplest single-field model (2) with  $\alpha = 1/3$ , which perfectly match the recent cosmological data, as shown in Fig. 2. Moreover, one can consider a more general superpotential,

$$W = \mu S f(Z) \tag{34}$$

obtain a more general potential

$$V = \mu^2 f^2 \left( \tanh \frac{\varphi}{\sqrt{2}} \right) \tag{35}$$

and show that for a very broad choice of the functions  $f(Z)$  this theory has the same observational predictions [34,36].

One may also consider the Kähler potential for general  $\alpha$ ,

$$K = -3\alpha \ln(1 - Z\bar{Z} - S\bar{S}) \tag{36}$$

and perform the same two-step procedure: construct dS space, and then deform it in the place corresponding to the end of inflation, e.g. at  $Z = 0$ . In order to do it, one may consider superpotentials

$$W = \mu S (1 - Z^2)^{\frac{3\alpha-1}{2}} \tag{37}$$

The geometry of the moduli space will be described by the Poincaré disk of the radius  $3\alpha$ . The potential of the field  $Z$  will be given by the cosmological constant  $\mu^2$ , but only for real values of the field  $Z$ , i.e. for  $\theta = 0$ . The potential has a stable minimum with respect to  $\theta$  at  $\theta = 0$  for  $\alpha > 1/3$ . In this case, the field  $\theta$  is frozen but the field  $\phi$  is free to move, so we can proceed the same way as before. Multiplying the superpotential by a function  $f(Z)$  so that  $W = \mu S f(Z) (1 - Z^2)^{\frac{3\alpha-1}{2}}$  results in a theory with the inflaton potential

$$V = \mu^2 f^2 \left( \tanh \frac{\varphi}{\sqrt{6\alpha}} \right) \tag{38}$$

and we recover a broad class of the single-field T-models and E-models discussed in Section 3.

Other examples of cosmological  $\alpha$ -attractors include supergravity models with a single inflaton field  $\varphi$  [35,14,40,51,52]. One may also modify the two-field models described above by considering different Kähler potentials and superpotentials, allowing stable inflation for  $\alpha < 1/3$ , breaking supersymmetry spontaneously and uplifting the minimum of the potential to account for the tiny vacuum energy (cosmological constant)  $V_0 \sim 10^{-120}$ , without altering the main cosmological predictions of  $\alpha$ -attractors [40,45].

This stability of the predictions with respect to even very significant changes of the potential is the main reason why we called these theories “cosmological attractors”: Their predictions for  $n_s$  and  $r$  are mostly determined by the underlying geometry of the moduli space rather than by the choice of the inflaton potential. That is why the knowledge of the geometry of the moduli space may be important for cosmology, even if the initial symmetry of the theory is hidden from us by spontaneous supersymmetry breaking and by the structure of the potential. This suggests that cosmological observations may help us to explore the geometric structure of the theory of all fundamental interactions.

## Acknowledgements

Maurits Cornelis Escher was a Dutch graphic artist. Some of his works were inspired by advanced developments in mathematics, some other works featured impossible constructions which tricked and misled our eye and imagination, and some were a combination of both. We are grateful to R. Bond, L. Page and U. Seljak for asking us about the meaning of the  $\alpha$ -parameter in our models, and for not being fully satisfied by our formal answer that it is inversely proportional to the curvature of the Kähler manifold. We are grateful to our collaborators S. Ferrara, M. Porrati and D. Roest for developing these cosmological models and to E. Bergshoeff, P. Binetruy, F. Bouchet, J.J. Carrasco, M. Gunaydin, S. Kachru, L. Senatore, E. Silverstein, A. Strominger, L. Susskind and A. Van Proeyen for many stimulating discussions. R.K. and A.L. are supported by the SITP and by the NSF Grant PHY-1316699. R.K. is also supported by the John Templeton Foundation grant ‘Quantum Gravity Frontiers,’ and A.L. is supported by the John Templeton Foundation grant ‘Inflation, the Multiverse, and Holography.’

## References

- [1] P.A.R. Ade, et al., BICEP2 and Planck Collaborations, A joint analysis of BICEP2/Keck array and Planck data, arXiv:1502.00612 [astro-ph.CO].
- [2] Planck Collaboration, P.A.R. Ade, et al., Planck 2015 results, XIII: cosmological parameters, arXiv:1502.01589 [astro-ph.CO]; P.A.R. Ade, et al., Planck Collaboration, Planck 2015, XX: constraints on inflation, arXiv:1502.02114 [astro-ph.CO].
- [3] A.D. Linde, Chaotic inflation, *Phys. Lett. B* 129 (1983) 177.
- [4] A.D. Linde, Particle Physics and Inflationary Cosmology, *Contemp. Concepts Phys.*, vol. 5, Harwood, Chur, Switzerland, 1990, p. 1, arXiv:hep-th/0503203, 1990.
- [5] A.A. Starobinsky, A new type of isotropic cosmological models without singularity, *Phys. Lett. B* 91 (1980) 99.
- [6] V.F. Mukhanov, G.V. Chibisov, Quantum fluctuation and nonsingular universe, *JETP Lett.* 33 (1981) 532 (in Russian) [*Pis'ma Zh. Eksp. Teor. Fiz.* 33, 549 (1981)].
- [7] A.H. Guth, The inflationary universe: a possible solution to the horizon and flatness problems, *Phys. Rev. D* 23 (1981) 347.
- [8] A.D. Linde, A new inflationary universe scenario: a possible solution of the horizon, flatness, homogeneity, isotropy and primordial monopole problems, *Phys. Lett. B* 108 (1982) 389.
- [9] A. Albrecht, P.J. Steinhardt, Cosmology for grand unified theories with radiatively induced symmetry breaking, *Phys. Rev. Lett.* 48 (1982) 1220.
- [10] A.A. Starobinsky, Dynamics of phase transition in the new inflationary universe scenario and generation of perturbations, *Phys. Lett. B* 117 (1982) 175; S.W. Hawking, The development of irregularities in a single bubble inflationary universe, *Phys. Lett. B* 115 (1982) 295; A.H. Guth, S.Y. Pi, Fluctuations in the new inflationary universe, *Phys. Rev. Lett.* 49 (1982) 1110; J.M. Bardeen, P.J. Steinhardt, M.S. Turner, Spontaneous creation of almost scale – free density perturbations in an inflationary universe, *Phys. Rev. D* 28 (1983) 679; V.F. Mukhanov, Gravitational instability of the universe filled with a scalar field, *JETP Lett.* 41 (1985) 493 [*Pis'ma Zh. Eksp. Teor. Fiz.* 41, 402 (1985)].
- [11] S.W. Hawking, A Brief History of Time, Bantam Books, NY, 1988.
- [12] A.D. Linde, Supergravity and inflationary universe, *Pis'ma Zh. Eksp. Teor. Fiz.* 37 (1983) 606 (in Russian) [*JETP Lett.* 37 (1983) 724]; A.D. Linde, Primordial inflation without primordial monopoles, *Phys. Lett. B* 132 (1983) 317.
- [13] L. Boubekeur, D.H. Lyth, Hilltop inflation, *J. Cosmol. Astropart. Phys.* 0507 (2005) 010, arXiv:hep-ph/0502047.
- [14] A.S. Goncharov, A.D. Linde, Chaotic inflation of the universe in supergravity, *Sov. Phys. JETP* 59 (1984) 930 [*Zh. Eksp. Teor. Fiz.* 86, 1594 (1984)]; A.B. Goncharov, A.D. Linde, Chaotic inflation in supergravity, *Phys. Lett. B* 139 (1984) 27.
- [15] A.A. Starobinsky, The perturbation spectrum evolving from a nonsingular initially De-Sitter cosmology and the microwave background anisotropy, *Sov. Astron. Lett.* 9 (1983) 302.
- [16] L.A. Kofman, A.D. Linde, A.A. Starobinsky, Inflationary universe generated by the combined action of a scalar field and gravitational vacuum polarization, *Phys. Lett. B* 157 (1985) 361.
- [17] B. Whitt, Fourth order gravity as general relativity plus matter, *Phys. Lett. B* 145 (1984) 176.
- [18] K. Freese, J.A. Frieman, A.V. Olinto, Natural inflation with pseudo-Nambu–Goldstone bosons, *Phys. Rev. Lett.* 65 (1990) 3233.
- [19] A.D. Linde, Axions in inflationary cosmology, *Phys. Lett. B* 259 (1991) 38; A.D. Linde, Hybrid inflation, *Phys. Rev. D* 49 (1994) 748, arXiv:astro-ph/9307002.
- [20] B.S. DeWitt, Quantum theory of gravity, 1: the canonical theory, *Phys. Rev.* 160 (1967) 1113.
- [21] A. Vilenkin, Creation of universes from nothing, *Phys. Lett. B* 117 (1982) 25.
- [22] A.D. Linde, The inflationary universe, *Rep. Prog. Phys.* 47 (1984) 925.
- [23] Y.B. Zeldovich, A.A. Starobinsky, Quantum creation of a universe in a nontrivial topology, *Sov. Astron. Lett.* 10 (1984) 135.
- [24] A. Vilenkin, Quantum creation of universes, *Phys. Rev. D* 30 (1984) 509.
- [25] A.D. Linde, Creation of a compact topologically nontrivial inflationary universe, *J. Cosmol. Astropart. Phys.* 0410 (2004) 004, arXiv:hep-th/0408164.
- [26] A. Vilenkin, The birth of inflationary universes, *Phys. Rev. D* 27 (1983) 2848.
- [27] A.D. Linde, Eternally existing self-reproducing chaotic inflationary universe, *Phys. Lett. B* 175 (1986) 395.
- [28] A.D. Linde, Eternal chaotic inflation, *Mod. Phys. Lett. A* 1 (1986) 81.
- [29] A.D. Linde, D.A. Linde, A. Mezhlumian, From the Big Bang theory to the theory of a stationary universe, *Phys. Rev. D* 49 (1994) 1783, arXiv:gr-qc/9306035.
- [30] R. Bousso, J. Polchinski, Quantization of four form fluxes and dynamical neutralization of the cosmological constant, *J. High Energy Phys.* 0006 (2000) 006, arXiv:hep-th/0004134.
- [31] S. Kachru, R. Kallosh, A.D. Linde, S.P. Trivedi, De Sitter vacua in string theory, *Phys. Rev. D* 68 (2003) 046005, arXiv:hep-th/0301240.
- [32] M.R. Douglas, The statistics of string/M theory vacua, *J. High Energy Phys.* 0305 (2003) 046, arXiv:hep-th/0303194.
- [33] L. Susskind, The Anthropic landscape of string theory, in: Bernard Carr (Ed.), *Universe or Multiverse?*, 2007, pp. 247–266, arXiv:hep-th/0302219.

- [34] R. Kallosh, A. Linde, Universality class in conformal inflation, *J. Cosmol. Astropart. Phys.* 1307 (2013) 002, arXiv:1306.5220 [hep-th];  
R. Kallosh, A. Linde, Multi-field conformal cosmological attractors, *J. Cosmol. Astropart. Phys.* 1312 (2013) 006, arXiv:1309.2015 [hep-th].
- [35] S. Ferrara, R. Kallosh, A. Linde, M. Porrati, Minimal supergravity models of inflation, *Phys. Rev. D* 88 (8) (2013) 085038, arXiv:1307.7696 [hep-th];  
S. Ferrara, P. Fré, A.S. Sorin, On the topology of the inflaton field in minimal supergravity models, *J. High Energy Phys.* 1404 (2014) 095, arXiv:1311.5059 [hep-th];  
S. Ferrara, P. Fré, A.S. Sorin, On the gauged Kahler isometry in minimal supergravity models of inflation, *Fortschr. Phys.* 62 (2014) 277, arXiv:1401.1201 [hep-th].
- [36] R. Kallosh, A. Linde, D. Roest, Superconformal inflationary  $\alpha$ -attractors, *J. High Energy Phys.* 1311 (2013) 198, arXiv:1311.0472 [hep-th];  
R. Kallosh, A. Linde, D. Roest, Large field inflation and double  $\alpha$ -attractors, *J. High Energy Phys.* 1408 (2014) 052, arXiv:1405.3646 [hep-th].
- [37] S. Cecotti, R. Kallosh, Cosmological attractor models and higher curvature supergravity, *J. High Energy Phys.* 1405 (2014) 114, arXiv:1403.2932 [hep-th].
- [38] M. Galante, R. Kallosh, A. Linde, D. Roest, The unity of cosmological attractors, *Phys. Rev. Lett.* 114 (14) (2015) 141302, arXiv:1412.3797 [hep-th].
- [39] A. Linde, Does the first chaotic inflation model in supergravity provide the best fit to the Planck data?, *J. Cosmol. Astropart. Phys.* 1502 (02) (2015) 030, arXiv:1412.7111 [hep-th].
- [40] R. Kallosh, A. Linde, Planck, LHC, and  $\alpha$ -attractors, arXiv:1502.07733 [astro-ph.CO].
- [41] D.S. Salopek, J.R. Bond, J.M. Bardeen, Designing density fluctuation spectra in inflation, *Phys. Rev. D* 40 (1989) 1753;  
F.L. Bezrukov, M. Shaposhnikov, The standard model Higgs boson as the inflaton, *Phys. Lett. B* 659 (2008) 703, arXiv:0710.3755 [hep-th].
- [42] S. Helgason, *Groups and Geometric Analysis (Integral Geometry, Invariant Differential Operators and Spherical Functions)*, Academic Press, New York, Orlando, 1984;  
R. Narayanan, C.A. Tracy, Holonomic quantum field theory of bosons in the Poincare disk and the zero curvature limit, *Nucl. Phys. B* 340 (1990) 568.
- [43] E. Silverstein, Simple de Sitter solutions, *Phys. Rev. D* 77 (2008) 106006, arXiv:0712.1196 [hep-th];  
E. Silverstein, A. Westphal, Monodromy in the CMB: gravity waves and string inflation, *Phys. Rev. D* 78 (2008) 106003, arXiv:0803.3085 [hep-th].
- [44] L. Susskind, *The Cosmic Landscape: String Theory and the Illusion of Intelligent Design*, Little, Brown and Company, 2005.
- [45] J.J. Carrasco, R. Kallosh, A. Linde, in preparation.
- [46] E. Cremmer, J. Scherk, S. Ferrara,  $SU(4)$  invariant supergravity theory, *Phys. Lett. B* 74 (1978) 61.
- [47] E. Bergshoeff, M. de Roo, B. de Wit, Extended conformal supergravity, *Nucl. Phys. B* 182 (1981) 173;  
M. de Roo, Matter coupling in  $N = 4$  supergravity, *Nucl. Phys. B* 255 (1985) 515.
- [48] S. Ferrara, R. Kallosh, A. Van Proeyen, Conjecture on hidden superconformal symmetry of  $N = 4$  supergravity, *Phys. Rev. D* 87 (2) (2013) 025004, arXiv:1209.0418 [hep-th].
- [49] E. Cremmer, B. Julia, The  $SO(8)$  supergravity, *Nucl. Phys. B* 159 (1979) 141;  
B. de Wit, H. Nicolai,  $N = 8$  supergravity, *Nucl. Phys. B* 208 (1982) 323.
- [50] M. Abreu, Kahler geometry of toric varieties and extremal metrics, *Int. J. Math.* 9 (6) (1998) 641–651;  
M. Abreu, Kahler metrics on toric orbifolds, *J. Differ. Geom.* 58 (1) (2001) 151–187;  
S. Donaldson, Scalar curvature and stability of toric varieties, *J. Differ. Geom.* 62 (2002) 289–349;  
S. Donaldson, Constant scalar curvature metrics on toric surfaces, *Geom. Funct. Anal.* 19 (1) (2009) 83–136.
- [51] D. Roest, M. Scalisi, Cosmological attractors from  $\alpha$ -scale supergravity, arXiv:1503.07909 [hep-th].
- [52] A. Linde, Single-field  $\alpha$ -attractors, arXiv:1504.00663 [hep-th].